PAPER

Clay-bionanocomposites with sacran megamolecules for the selective uptake of neodymium†

Ana C. S. Alcântara,[a] Margarita Darder,[a] Pilar Aranda,[a] Seiji Tateyama,[b] Maiko K. Okajima,[b] Tatsuo Kaneko,[b] Makoto Ogawa[c] and Eduardo Ruiz-Hitzky*[a]

Sacran, an anionic megamolecular polysaccharide extracted from the cyanobacterium *Aphanothece sacrum*, is an interesting biopolymer for developing functional clay-based bionanocomposites due to its colloidal and metal complexing properties. This work introduces novel bionanocomposites based on the assembly of sacran to sepiolite, a fibrous hydrated magnesium silicate, reporting some of their special features. Sacran–sepiolite films show tensile moduli about twice that of neat sacran films, and improved resistance and integrity in aqueous solutions. These materials can act as adsorbents of lanthanide ions, profiting from the well-known adsorption properties of sepiolite and the ability of sacran to complex rare earth and heavy metal ions. Sacran–sepiolite materials show a clear preference for Nd^{3+} ions over Ce^{3+}, Eu^{3+} and Gd^{3+}, and the results confirm the influence of the conformation of sacran chains in crystalline domains on the adsorption properties. In fact, only those materials prepared from concentrated sacran solutions, with the polysaccharide chains arranged as liquid crystals, and involving around 27% (w/w) of sepiolite showed a remarkable synergistic effect on the retention of Nd^{3+} ions, being promising as biosorbents for the effective and selective recovery of neodymium from aqueous media.

Introduction

Bionanocomposite materials, a group of organic–inorganic hybrid materials involving naturally occurring polymers and inorganic solids that show at least one dimension at the nanometer scale, can exhibit improved structural and functional properties together with biocompatible and biodegradable character associated with the biopolymer.[1–3] The biocompatibility and the eco-friendly character are specially attained when natural clay is used as the inorganic counterpart. The main research in this area was initially focused on the combination of clay, with lamellar or fibrous morphology, with the most abundant polymers on earth (cellulose, chitosan, starch), and it is being currently enlarged with the use of biopolymers derived from alternative sources, as those produced by microorganisms, such as microbial or bacterial polysaccharides[4,5] and polyesters.[6]

Sacran, a novel polysaccharide extracted from the edible blue-green cyanobacteria *Aphanothece sacrum*,[7] is an attractive biopolymer for the development of novel bionanocomposites based on its assembly to inorganic solids. This anionic polysaccharide consisting of both carboxylate and sulphate groups shows very interesting features regarding its extremely high molecular weight (about 1.6×10^7 g mol^{-1}), its gelation ability through adsorption of heavy metal ions,[8] or its ability to self-orientate depending on the concentration. This latter property allows the sacran chains to arrange as rigid rods in a helical conformation when the concentration is between 0.09 and 0.25% (w/v), to form gels at a concentration between 0.25 and 0.5% (w/v), and even to adopt a liquid crystalline state in solutions at a concentration higher than 0.5% (w/v).[9]

The current work introduces novel bionanocomposite materials based on the assembly of sacran and sepiolite, an hydrated magnesium silicate with fibrous morphology and the theoretical unit cell formula $Si_{12}O_{30}Mg_8(OH,F)_4(H_2O)_4 \cdot 8H_2O$.[10] This silicate has a large specific surface area, *ca.* 320 m^2 g^{-1}, and microporosity due to its unique structure, showing the alternation of blocks and tunnels growing up in the fibre direction.[11,12] Another interesting feature is the presence of silanol groups (Si-OH) located at the external edges of the blocks, which can be involved in the interactions with organic and biological species or can be functionalized through covalent grafting of

[a]*Instituto de Ciencia de Materiales de Madrid, CSIC, 28049 Madrid, Spain. E-mail: eduardo@icmm.csic.es*

[b]*School of Materials Science, Japan Advanced Institute of Science and Technology, 1-1 Asahidai, Nomi, Ishikawa 923-1292, Japan*

[c]*Department of Earth Sciences, Waseda University, Nishiwaseda 1, Tokyo 169-8050, Japan*

This journal is © The Royal Society of Chemistry 2014

J. Mater. Chem. A, 2014, **2**, 1391–1399 | **1391**

diverse organic groups. In a similar way to commonly used layered silicates, sepiolite has been applied as a nanofiller of polymers and biopolymers in the development of nano-composite materials,[12–14] providing in many cases better mechanical properties than those achieved with layered silicates, which can be attributed to the high aspect ratio of the sepiolite fibres or to their exceptional interaction with the polymer chains.[15]

The first target of the current work has been to elucidate the interactions established between sacran and sepiolite fibres and to explore their influence on the new properties of the resulting bionanocomposites, with special interest in the adsorption properties of these functional materials. Biosorption of organic and inorganic pollutants by microbial biomass and polysaccharides extracted from microbial cells has been widely studied for water remediation,[16,17] and exopolysaccharides extracted from bacteria have been successfully applied in the removal of heavy metal ions[18] and lanthanide ions.[19] Similarly, recent studies revealed the ability of sacran to complex very heavy metal ions forming gels.[8,20,21] This adsorption property is also expected in sacran–sepiolite materials, as already confirmed for the anionic sacran-MWCNT complexes recently reported,[22] which retained the gelation behaviour of sacran by lanthanide adsorption after assembling the nanotubes. In this way, the efficiency of the sacran–sepiolite bionanocomposites towards the uptake of lanthanide ions, with special emphasis on neodymium, will be evaluated. The significance of the Nd recovery processes can be easily evidenced as in the last decade there has been a remarkable increase not only in the number of reports on neodymium but also in the commercial demand of this element. Neodymium is receiving key applications in NdFeB (NIB) permanent magnets, being the strongest commercially available magnets with applications in computer hard drives, microphones and hearing aids, cell phones, motors and wind turbines, hybrid cars, toys, *etc.*[23] Nd-doped yttrium-aluminium-garnet (YAG) lasers are powerful tools used in biomedicine (skin cancer treatment), industry (cutting steel), and advanced military weaponry.[24] Other important applications refer to neodymium as a colouring agent for glasses and ceramics[23] as well as efficient Ziegler/Natta catalysts for diene polymerization.[25] Therefore, the development of new materials acting as efficient Nd complexing systems represents a suitable strategy for the recovery and further use of this valuable element.

Experimental

Starting materials and reagents

Sacran (Scr) was extracted from frozen samples of the cyanobacteria *A. sacrum* by a previously reported method.[7,26] Sepiolite (Sep) from Vicálvaro (Spain) commercialized as Pangel® S9 was provided by TOLSA S.A. Neodymium(III), gadolinium(III) and europium(III) chloride salts (99% metals basis) were supplied by Sigma-Aldrich and cerium(III) nitrate hexahydrate (99.9% Ce) was from ABCR. Deionized water (resistivity of 18.2 MΩ cm) was obtained with a Maxima Ultrapure Water from Elga.

Preparation of sacran–sepiolite bionanocomposites

A set of solutions with different sacran concentrations was prepared in 50 mL of water by means of an ultrasound tip (VC750 Sonics Vibra Cell, operating at 20 kHz), using a tip of 13 mm and applying intermittent pulses of 10 s followed by a standby step of 10 s up to a total applied energy of 10 kJ. In this way, sacran solutions with the concentration ranging between 0.02 and 1.26% (w/v) were obtained (Table 1). Sepiolite dispersions were prepared in water by applying magnetic stirring to properly disperse the clay. Sepiolite dispersions (50 mL) were gradually added to each sacran solution under magnetic stirring, forming a single batch that is then kept under constant stirring for 48 h at 30 °C (±2 °C) in an incubator shaker at 100 rpm. The resulting dispersion was placed on a glass plate and allowed to dry at room temperature and atmospheric pressure, achieving self-standing biohybrid films.

In order to study the adsorption behaviour of sacran on sepiolite by means of the corresponding adsorption isotherm, an aliquot (50 mL) of sacran solutions with variable concentrations (0.02–0.1% (w/v)) was mixed with 50 mL of an aqueous dispersion containing 150 mg of sepiolite. The sacran–sepiolite dispersions were stirred at 30 °C for 48 h and then centrifuged in order to remove the excess of sacran not assembled to sepiolite. The separated solids were dried in an oven at 40 °C overnight, yielding in this case particulate biohybrid materials.

Characterization

Fourier transform infrared (FTIR) spectra were recorded with the FTIR spectrophotometers BRUKER IFS 66v/S and NICOLET-20SXC. Each sample was placed in the sample holder as a film and scanned from 4000 to 500 cm^{-1} with 2 cm^{-1} resolution. The amount of organic matter in the fibrous clay was determined by CHNS elemental chemical microanalysis using a LECO-CHNS-932 analyzer. The thermal behaviour of the different prepared materials was analyzed from the simultaneously recorded thermogravimetric (TG) and differential thermal analysis (DTA) curves using SEIKO SSC/5200 equipment, in experiments carried out under air atmosphere (flux of 100 mL min^{-1}) from

Table 1 Sacran–sepiolite bionanocomposite films containing variable amounts of sacran and sepiolite. The numbers in the sample codes indicate the percentage of sepiolite in each bionanocomposite material

Sample codes	Initial concentration of sacran, % (w/v)	% of each component in the final material	
		Sacran	Sepiolite
Scr–Sep2	1.26	98	2
Scr–Sep5	1.22	95	5
Scr–Sep10	1.16	90	10
Scr–Sep15	1.10	85	15
Scr–Sep20	1.04	80	20
Scr–Sep27	0.80	73	27
Scr–Sep43	0.40	57	43
Scr–Sep50	0.30	50	50
Scr–Sep75	0.10	25	75
Scr–Sep83	0.060	17	83

1392 | *J. Mater. Chem. A*, 2014, **2**, 1391–1399

This journal is © The Royal Society of Chemistry 2014

room temperature to 1000 °C at 10 °C min^{-1} heating rate. Solid-state ^{13}C CP MAS NMR spectra were obtained on a Bruker Avance 400 spectrometer, using a standard cross-polarization pulse sequence. Samples were spun at 10 kHz. A contact time of 2 ms and a period between successive accumulations of 5 s were used. The number of scans was 800. Chemical shift values were referenced to tetramethylsilane (TMS). Surface morphology was observed using FE-SEM equipment FEI-NOVA NanoSEM 230, equipped with an EDX detector from EDAX-Ametek that allowed semi-quantitative analysis of elements. Sample preparation was performed by adhering particle samples on a carbon tap for direct observation without the requirement of any conductive coating on the surface. The viscosity of sacran solutions was determined using a Brookfield viscometer and the presence of crystalline domains was detected by means of the polarizing microscope Eclipse LV100POL from Nikon. Absolute weight-average molecular weights of the sacran samples were measured using a size exclusion chromatography multi-angle laser light scattering (SECMALLS) system. The chromatographic system was a SHODEX GPC consisting of a pump and an Alliance autosampler. Three columns, a Shodex OHpak (8.0 mm ID × 300 mm length) SB-807G (Guard), a SB-807 HQ, and an SB-804 HQ, were used. The column temperature was kept at 40 °C. The eluent was NaNO$_3$ aqueous solution (0.1 M) at a flow rate of 1 mL min^{-1}. The sample solution (injected volume: 100 mL, concentration: 0.01 wt%) was filtered using a filter with a pore size of 5 μm just before the measurement. The light scattering instrument, a DAWN Heleos II multiangle laser light scattering detector (detector angles: 13.0, 20.7, 29.6, 37.5, 44.8, 53.1, and 61.1°) from Wyatt Technology, operating at 665.2 nm, was placed between the SEC and a precise refractive index (RI) detector (Wyatt Technology Optilab T-rEX; laser wavelength (658.0 nm)). The DAWN detector was calibrated with toluene and normalized using a pullulan standard with a molecular weight of 22 000 g mol^{-1}. The dn/dc value for sacran was 0.108 mL g^{-1} (25 °C), as determined using the RI machine Optilab T-rEX.

Mechanical properties

Mechanical properties such as the tensile modulus (E) and percent elongation at break (E.B) of the film samples were evaluated with a Model 3345 Instron Universal Testing Machine (Instron Engineering Corporation Canton, MA, USA) according to the ASTM standard method D 882-88. Rectangular samples (*ca.* 60 mm × 15 mm) were mounted between the grips with an initial separation of 50 mm, and the cross-head speed was set at 2 mm min^{-1}. Three replicates were run for each film treatment.

Dynamic vapour sorption

Water vapour sorption of the sacran–sepiolite materials was measured gravimetrically using Aquadyne DVS equipment (Quantachrome Instruments). The weight of the samples in powder form was constantly monitored at 25 °C and recorded as the relative humidity was automatically varied between 0 and 95% by the blending of dry N$_2$ carrier gas with a water saturated gas stream. Samples were initially dried *in situ* at 80 °C in a flow of dry gas in order to know the weight of the dry samples.

Sorbed moisture was expressed as grams of water retained by 100 g of dry sample.

Uptake of lanthanides by sacran–sepiolite bionanocomposite films

A weighed part of each sacran–sepiolite film (12.5 mg) was added as an adsorbent to reaction flasks containing 6.25 mL of 10^{-1} M aqueous solution of lanthanide ions. All the systems were maintained at 25 ± 2 °C in an incubator shaker at 100 rpm. After 24 h the supernatants were taken and the amount of non-adsorbed metal ions remaining in solution was determined spectrophotometrically. For this purpose, the spectra of the supernatant solutions were measured in the UV-visible range, at wavelengths between 200 and 800 nm, using a UV spectrophotometer (Shimadzu, UV1201 model) and quartz cuvettes with 1 cm path length. The amount of metal ions adsorbed per gram of the material was calculated from the difference between the initial and the final amount of lanthanide ions in each solution.

Results and discussion

Preparation of the sacran–sepiolite bionanocomposites

Usually aqueous sacran solutions are prepared in hot distilled water at 90 °C for more than 10 h as previously reported.[8] This represents a limitation for rapid preparation of the starting solutions required for the assembly of sacran to the sepiolite fibrous clay. To speed up this step, homogenous sacran solutions were easily and quickly prepared in this work by means of an ultrasound tip. This procedure led to solutions with lower viscosity than those prepared in hot water, which showed a value of 880 cP at 24.3 °C for a 0.3% (w/v) sacran concentration. With sonication, the viscosity of this sacran solution decreased considerably as the applied energy was raised, up to values around 25 cP (Fig. S1A†), pointing to a possible damage of the sacran chains. Thus, size exclusion chromatography was applied to the sonicated sacran solutions in order to check the molecular weight (Fig. S1B†). The results suggested that in fact the energy applied during sonication was able to provoke a partial break of the sacran chains, but it was also confirmed that the molecular weight of sonicated chains under the applied conditions maintained very high values over 10^6 g mol^{-1}, being still possible to consider them as megamolecules. In addition, transmittance measurements of sonicated solutions showed the tendency of sacran chains to reorganize in a short time. This fact was revealed by the loss of transparency of a highly concentrated sacran solution with increasing time, leading to an opaque solution with only 10% of transmittance in less than one day (Fig. S2†). This optical behaviour was attributed to the formation of a liquid crystal phase by self-organization of sacran chains in concentrated solutions,[9] as observed in other lyotropic liquid crystalline polymer gels.[27] The presence of crystalline domains in a concentrated sacran solution (0.8% (w/v)) prepared by ultrasonication was confirmed by using a polarizing microscope, as shown in Fig. S3.† These results indicated a similar organization of the ultrasonicated sacran chains to that proposed for analogous solutions prepared by

This journal is © The Royal Society of Chemistry 2014

J. Mater. Chem. A, 2014, **2**, 1391–1399 | **1393**

magnetic stirring.[9] In contrast, sacran chains in diluted solutions adopted a random-coil conformation both in the original and sonicated state, remaining transparent as the time increases (Fig. S2†).

The assembly of the sonicated sacran and the fibrous silicate sepiolite was carried out by mixing both components in aqueous solution under conventional magnetic stirring, varying the sacran concentration as well as the sepiolite content in order to obtain a set of bionanocomposite materials with a wide range of sacran–sepiolite mass ratios (Table 1). In order to study the affinity between the polysaccharide and the fibrous silicate, the adsorption isotherm of sacran on sepiolite at 30 °C was investigated. The shape of the isotherm shown in Fig. 1 indicated that the polysaccharide was almost completely adsorbed at low initial concentration. According to the Giles classification of isotherms,[28] this type of isotherm was defined as the H-type isotherm, a special case of the Langmuir isotherm, which indicated a high affinity of the sacran adsorbate to the sepiolite substrate. In the current isotherm, it was also possible to appreciate a plateau region starting from an equilibrium concentration around 100 mg L^{-1}, which corresponded to a maximum amount of 4.5 g of sacran adsorbed per 100 g of sepiolite. At these values, a complete coverage of the surface of fibrous silicate by the sacran molecules was achieved, showing a monolayer-type conformation on the surface of the sepiolite fibres.

The molecular interactions that take place between the silicate and the polysaccharide, as well as the degree of coverage of the silicate by sacran molecules were also investigated by FTIR spectroscopy. Fig. 2 shows the spectra in the 4000–500 cm^{-1} wavenumber range of the starting components as well as those of two selected bionanocomposites. The spectrum of sacran (Fig. 2a) exhibited the characteristic bands at 1640 cm^{-1}, 1421 cm^{-1}, 1247 cm^{-1} and 1043 cm^{-1} that are attributed to ν_{CO} (C=O) of amide I, ν_{CO} (COO), ν_{SO} (S=O) of SO$_4$ and ν_{CO} (C–O–C) vibrations, respectively.[7] In the same spectrum, the stretching vibration bands at ~2932–2892 cm^{-1}, assigned to CH groups, can be also distinguished. Some of these bands can be easily appreciated around 2920, 1420 and 1240 cm^{-1} in the spectra of the bionanocomposites together with other characteristic
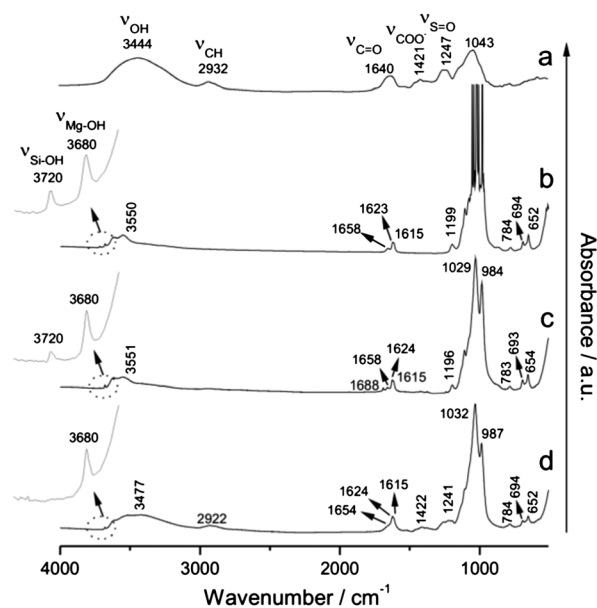
Fig. 2 FTIR spectra (4000–500 cm^{-1}) of pure sacran (a), sepiolite (b), Scr–Sep85 (c) and Scr–Sep50 (d) recorded on the samples processed as films.

bands of sepiolite (Fig. 2c and d). As a source of information regarding the nature of the interactions between the sepiolite and biopolymers,[15,29,30] the bionanocomposite spectra were usually analyzed taking into account the vibrations of silanol groups (Si-OH), located at the external surface of the silicate, as well as those of Mg-OH groups, located inside the tunnels of sepiolite. In the current study, these bands of structural hydroxyl groups in the starting sepiolite (Fig. 2b) appeared at 3720 and 3680 cm^{-1}, respectively. However, the IR spectra of oriented films of Scr–Sep85 (Fig. 2c) and Scr–Sep50 (Fig. 2d) showed a strong decrease in the intensity of the band assigned to the OH stretching vibration (ν_{O-H}) of the Si-OH silanol groups as the amount of sacran increases in the hybrid material, making this band practically unappreciable in the Scr–Sep50 biohybrid material. A possible explanation for this observation is the strong interaction through hydrogen bonding between the accessible sacran groups and the hydroxyl groups of the silicate surface, which leads to the shift of the ν_{Si-OH} band towards lower frequency values.[11,29,30] On the other hand, the ν_{O-H} vibration band assigned to Mg-OH groups in the clay structure typically appearing at around 3680 cm^{-1} remained unaltered, even at high amounts of adsorbed sacran. As discussed above, these groups are located inside the block structure of the sepiolite, becoming inaccessible to the adsorbed sacran chains.

Another important set of hydroxyl stretching bands typical in the untreated sepiolite (Fig. 2b), corresponded to the intensive broad band assigned to the bending vibration modes of zeolitic and coordinated water molecules at 1658 cm^{-1} and 1623 cm^{-1}, respectively.[11] Generally, perturbation in the frequencies of these bands, reflected in a shift towards higher frequencies and a decrease of the intensity of the component at lower wavenumbers, has been ascribed to the existence of hydrogen-bonding interactions with adsorbed species within the tunnels
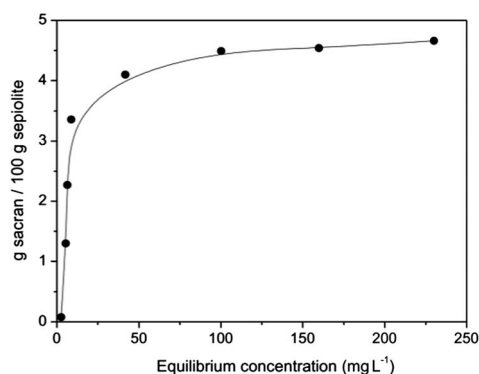

Fig. 1 Adsorption isotherm at 30 °C of sacran from aqueous solution on sepiolite. Adsorption amounts were deduced from CHNS chemical analyses of the bionanocomposite solids.
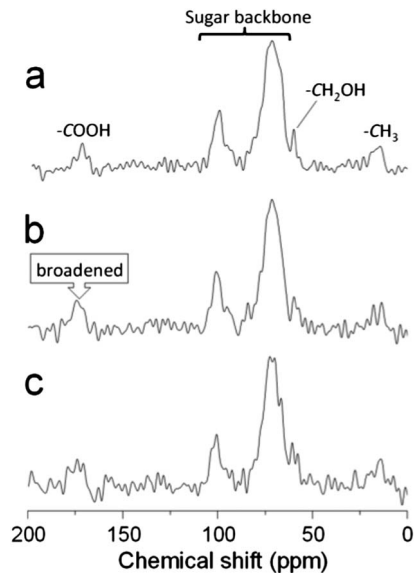
1394 | J. Mater. Chem. A, 2014, 2, 1391–1399

This journal is © The Royal Society of Chemistry 2014

Fig. 3 ^{13}C NMR spectra of (a) pure sacran and the bionanocomposites (b) Scr–Sep27 and (c) Scr–Sep50.

Fig. 4 FE-SEM images of sacran (a) and the bionanocomposites Scr–Sep50 (b) and Scr–Sep27 (c).

of sepiolite.[31] In the spectra of bionanocomposites (Fig. 2c and d), these bands seem to remain unperturbed even when the amount of sacran in the material is high (Fig. 2d), being in this latter case partially overlapped with the characteristic amide I band of sacran at 1640 cm^{-1}.

Solid state ^{13}C NMR spectra of pristine sacran (Fig. 3a) showed signals at 15–25 ppm, *ca.* 62 ppm, 65–110 ppm, and 170–180 ppm that were assigned to the C-6 methyl group of deoxyl hexoses (–CH_3), C-6 hydroxymethyl of hexoses (–CH_2OH), sugar backbones, and carboxyl groups (–$COOH$), respectively. In both the Scr–Sep bionanocomposite samples analyzed in this NMR study (Fig. 3b and c), the signal/noise ratio was too low to analyze in detail the spectra due to the sacran dilution in these materials. Low intensity signals of the C-6 methyl group of deoxyl hexoses and C-6 hydroxymethyl of hexoses were split into several peaks. On the other hand, the signals assigned to carboxyl groups in the Scr–Sep27 spectrum were broadened, indicating a decrease in their spin–spin relaxation time (T_2) due to the suppressed molecular mobility around the carbon atom of these carboxylic groups. Carboxylic functions in sacran have been associated with the binding sites for metal ions as already reported,[8] so these results could point to a possible effect of the assembling of sacran to sepiolite, affecting the metal binding sites presumably due to the carboxylate interaction with the sepiolite surface.

The FE-SEM images of neat sacran (Fig. 4a) reveal a curious morphology consisting of thin layers and small fibrils. However, the sacran–sepiolite hybrid materials showed a quite different morphology compared to sacran alone. In both cases, Scr–Sep50 (Fig. 4b) and Scr–Sep27 (Fig. 4c) bionanocomposites exhibited a more compact morphology, where the sepiolite fibres seem to be well integrated within the biopolymer structure. Such arrangement of the silicate fibres and the polysaccharide could indicate an enhancement of the mechanical properties of these hybrid materials.
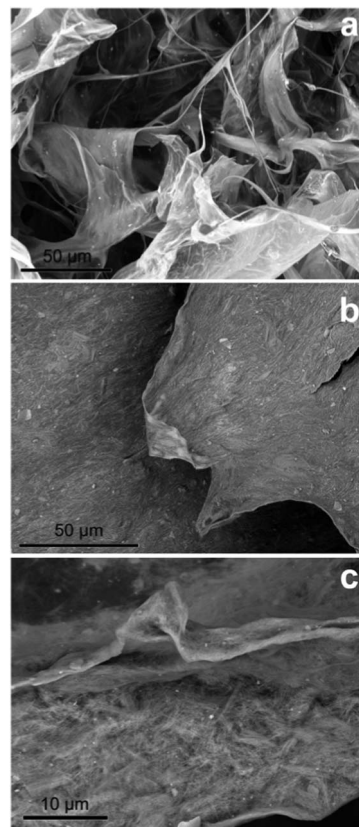
Properties of sacran–sepiolite bionanocomposite films

Thermal behaviour. DTA and TG curves recorded in the 20–900 °C range under air flow conditions (Fig. 5) confirm the thermal stability of the sacran–sepiolite bionanocomposite films in comparison with the biopolymer alone. The DTA curve corresponding to the pristine sacran (Fig. 5a) shows an endothermic process at 50 °C and four exothermic processes at 272, 326, 365 and 505 °C, respectively. The first one, associated with a weight loss of 9.6% in the TG curve, is attributed to the elimination of adsorbed water molecules. The exothermic processes from 270 until approximately 500 °C, which present a total mass loss of 63.6%, can be related to the pyrolytic decomposition followed by the combustion of the biopolymer.

The neat sepiolite (Fig. 5b) shows a mass loss with endothermic peaks at 75 and 278 °C, associated with the loss of the physically adsorbed (weight loss 11.5%) and zeolitic water molecules (weight loss 3.0%). The slightly endothermic process observed at 505 °C (weight loss 2.5%) and the exothermic process observed at 830 °C (weight loss 3.1%) are attributed to the loss of water molecules within the structural tunnels and the internal dehydroxylation of sepiolite to become proto-enstatite.[32] In the thermogram of the Scr–Sep27 hybrid sample (Fig. 5c), which is quite similar to that of the starting sacran, the DTA peaks corresponding to sacran decomposition have been shifted toward higher temperature values, appearing at 358 and 452 °C and associated with weight losses of 15 and 8.2%,
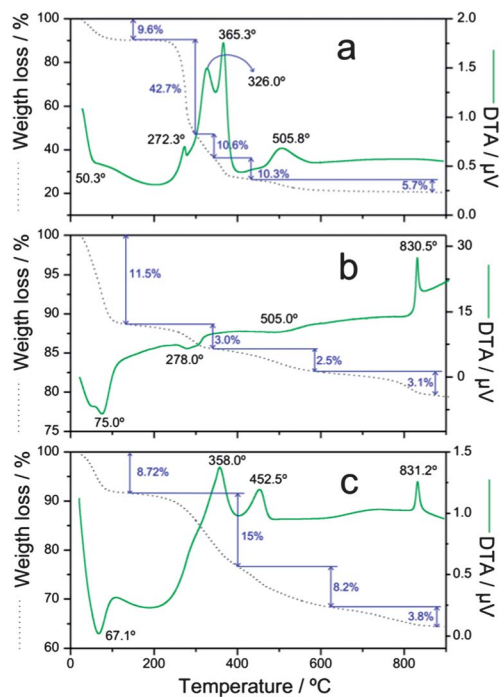
This journal is © The Royal Society of Chemistry 2014

J. Mater. Chem. A, 2014, **2**, 1391–1399 | **1395**

Fig. 5 TG and DTA curves obtained for sacran (a), sepiolite (b), and Scr–Sep27 bionanocomposite (c).

respectively. These increases in temperature suggest an improvement in the thermal stability of the resulting sacran–sepiolite bionanocomposites. The water content in the Scr–Sep27 bionanocomposite is 8.2% at approximately 67 °C. The DTA peak at 831 °C corresponds to the dehydroxylation process of the residual sepiolite.[32]

Mechanical properties. Tensile stress studies were carried out in order to evaluate the effect of the sepiolite fibres on the mechanical properties of the sacran films. The values of tensile modulus and elongation-at-break of a set of bionanocomposites are collected in Table 2 together with those measured for the unmodified sacran film. All the biohybrid samples show higher tensile modulus than that of pristine sacran films, even in those materials with high filler content, indicating the increase of the material stiffness due to the addition of the filler. In most cases, the measured modulus is around twice that of the sacran film (0.9 GPa), or even a bit higher in the bionanocomposite with a 15% of sepiolite, which shows a tensile modulus of 2.2 GPa.

Concerning the elongation-at-break values of the bionano-composites, a decrease is observed with respect to the value

measured for the neat sacran film, 20.2%, indicating a reduction in the plastic behaviour of all these samples. The values remain constant (around 9%) in samples with filler amounts higher than 15%. The decrease with respect to the neat biopolymer can be attributed to the reduced mobility of the sacran chains after assembling the sepiolite fibres, as observed for some clay-reinforced polymers.[12,33] However, the strong interaction between sacran and sepiolite, confirmed from spectroscopic techniques, allows the preparation of resistant self-supporting films provided with good tensile modulus, which can be easily handled even after immersion in aqueous media.

Dynamic water sorption. While pristine sacran films immersed in water swelled and disintegrated rapidly, the stability and resistance of the sacran–sepiolite materials in aqueous media were considerably improved. A water vapour sorption analysis of these films confirmed the tendency of sacran to absorb a larger amount of water than its sepiolite-based bionanocomposites (Fig. S4A†). Curiously, all the hybrid samples showed lower tendency towards water sorption than both individual components, being Scr–Sep27 the sample with the lowest water retention capacity. This fact could be attributed to the blockage of hydroxyl groups in both components after the assembly of the fibrous silicate and the biopolymer, which reduces the available sites for water adsorption. Focusing on the first part of the isotherm (Fig. S4B†), the fitting of these data to the Langmuir model (Table S1†) shows a decrease in the Langmuir capacity constant (X_m in eqn (S1†)) of neat sacran (31.6 g H_2O/100 g dry mass) to values of 11.1, 11.6 and 13.2 g H_2O/100 g dry mass for the Scr–Sep27, Scr–Sep50 and Scr–Sep83 bionanocomposites, respectively. The A_L value of the Scr–Sep83 materials is very close to that of the pristine sepiolite, 13.1 g H_2O/100 g dry mass, showing similar water sorption isotherms for both samples.

Adsorption properties of sacran–sepiolite materials

The sacran–sepiolite bionanocomposites were evaluated as adsorbents of lanthanide ions, with the aim to profit from the well-known ability of sacran to complex rare earth ions and other heavy metal ions.[8,20,21] Batch experiments were carried out with the set of samples detailed in Table 1, and using 6.25 mL of
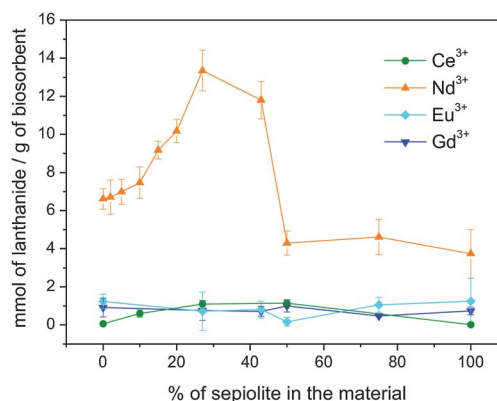
Table 2 Tensile properties of the sacran–sepiolite bionanocomposite materials. E = tensile modulus and E_B = elongation at break

Sacran–sepiolite sample	E (GPa)	E_B (%)
Scr	0.92 ± 0.10	20.2 ± 2.20
Scr–Sep5	1.93 ± 0.10	11.9 ± 1.24
Scr–Sep15	2.21 ± 0.03	8.27 ± 0.78
Scr–Sep27	2.01 ± 0.02	9.98 ± 1.10
Scr–Sep50	1.93 ± 0.07	9.14 ± 0.96
Scr–Sep75	1.90 ± 0.05	8.56 ± 1.25

Fig. 6 Uptake of lanthanide(III) ions by sacran–sepiolite bionano-composites with variable content of sepiolite.

1396 | J. Mater. Chem. A, 2014, 2, 1391–1399

This journal is © The Royal Society of Chemistry 2014

10^{-1} M aqueous solutions of some selected lanthanides, such as Ce(III), Nd(III), Gd(III), and Eu(III). The increased stability in water of sacran–sepiolite materials in comparison with neat sacran avoids their dissolution during the adsorption study. The amount of adsorbed lanthanide ions was determined spectrophotometrically from the difference between the concentration of the starting solution and that of the supernatant after the adsorption process. The results shown in Fig. 6 confirmed the ability of all the tested materials to adsorb high amounts of Nd^{3+} ion in comparison with Ce^{3+}, Gd^{3+} and Eu^{3+} ions.

The different uptake of the tested ions could be attributed to the increased rigidity of the coordination complex formed in the sacran–sepiolite materials, which can reduce the stability constants and increase the lanthanide(III) size selectivity of the complexing agent due to the slightly different ionic radius of the tested ions, as proven for other types of ligands.[34] In this case, the size of Nd^{3+} seems to match well with the bionanocomposite cation-exchangeable sites, leading to an increased stability in the complexation of these ions and consequently to a higher uptake. The uptake results confirm that the assembly of sacran chains to the sepiolite fibres does not hamper totally their ability to adsorb lanthanide ions, in spite of the possible blockage of the sacran carboxylate groups due to their interaction with the sepiolite surface, as suggested from the solid state NMR study. A similar finding has already been reported by Okajima *et al.*[22] for sacran/carbon nanotube dispersions that retained the sacran's ability to form gel beads when dropped into lanthanide ion solutions. In the present case, the affinity of sacran towards neodymium was only reduced with respect to that of neat sacran in samples with higher content of sepiolite (>50% (w/w)). Interestingly, a synergistic effect was observed in samples with the sepiolite content between 10 and 40%, showing a maximum adsorption of 13.4 mmol of Nd^{3+} per g of sorbent in the sample containing 27% of sepiolite. This value was considerably higher than other reported values in the literature for a wide variety of sorbent materials, including those derived from biomass, such as *Sargassum* sp. extracted from brown seaweed (0.7 mmol Nd^{3+} per g),[35] DNA-filter hybrids (1.3×10^{-3} mmol Nd^{3+} per g)[36] and *O*-carboxymethyl chitosan/silica hybrids (0.4 mmol Nd^{3+} per g),[37] or other conventional sorbents such as activated charcoal (0.8 mmol Nd^{3+} per g),[38] or the D113-III ion-exchange resin (1.8 mmol Nd^{3+} per g).[39] FESEM and EDX analysis of the Scr–Sep27 sample after the uptake process (Fig. 7) confirmed the homogeneous distribution of the Nd^{3+} ions along the whole sacran–sepiolite material, providing an indication of the homogeneity of this bionanocomposite.

The study was then focused on those samples affording the highest adsorption of Nd^{3+} ions, with the aim to find out the origin of such enhanced affinity. Analogous bionanocomposites with 27% sepiolite, but using other polysaccharides extracted from algae, carboxylate-bearing alginate and sulphate-bearing carrageenan, were prepared for comparison with the sacran-based sample. However, none of them showed the synergistic behaviour observed for the Scr–Sep27 sample, affording in both cases similar values for adsorbed Nd^{3+} ions to the corresponding neat alginate or carrageenan polysaccharides (Fig. S5†). This result corroborates that both carboxylate and sulphate groups
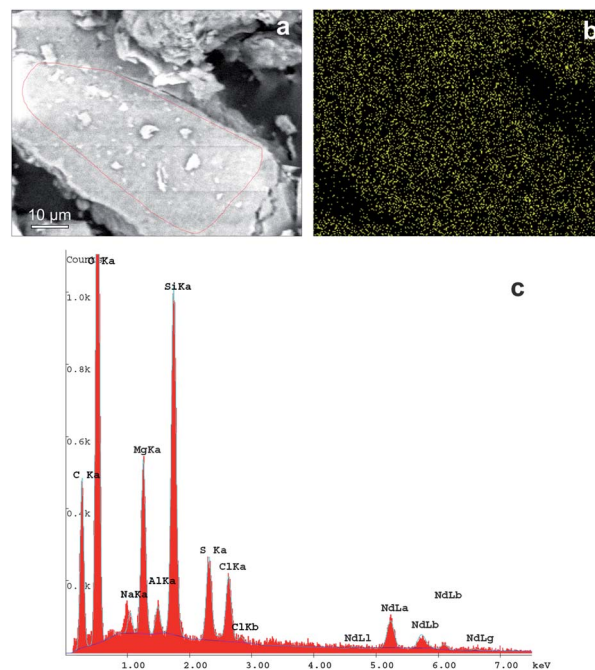

Fig. 7 FESEM image (a), Nd(III) elemental map (b) and EDX analysis (c) of the Scr–Sep27 bionanocomposite after neodymium uptake, revealing the presence and homogeneous distribution of Nd^{3+} ions in the material.

in the sacran structure can contribute to the Nd^{3+} uptake, but it does not clarify about the observed synergistic effect.

Previous studies carried out by Okajima *et al.*[9] reported the ability of sacran chains to self-organize depending on the concentration. At values higher than 0.5% (w/v), sacran chains are self-organized forming liquid crystal arrangements. It was also found that this liquid-crystalline state had a strong influence on the gelation behaviour of sacran upon addition of very heavy metal ions,[8] including the series of lanthanides. Based on these previous findings and considering the fact that the Scr–Sep27 sample showing the highest uptake of Nd^{3+} ions was prepared from a 0.8% (w/v) starting sacran solution (Table 1), the preservation of the liquid-crystalline state in the bionanocomposites was suggested as the possible origin of the marked affinity for neodymium. Fig. S6† shows the organization of sacran chains in each one of the starting solutions used in the preparation of the samples tested for the neodymium uptake.

In order to confirm this hypothesis, three sets of bionanocomposite materials with starting sacran solution of fixed concentration (0.05, 0.3 or 0.8% (w/v)) were prepared with sepiolite contents of 10, 27, 50 and 75% for each group of samples, and the neodymium uptake with the resulting materials was carried out under the same conditions as the previous test. Interestingly, from Fig. 8 it can be confirmed that the sacran–sepiolite sample with 27% of clay only had a huge affinity towards Nd^{3+} ions when it was prepared from a high sacran concentration (0.8% (w/v)). At the same time, the results proved that the maximum adsorption did not only depend on the sacran concentration, but it was uniquely achieved for an optimal content of sepiolite, around 27%. In contrast, the
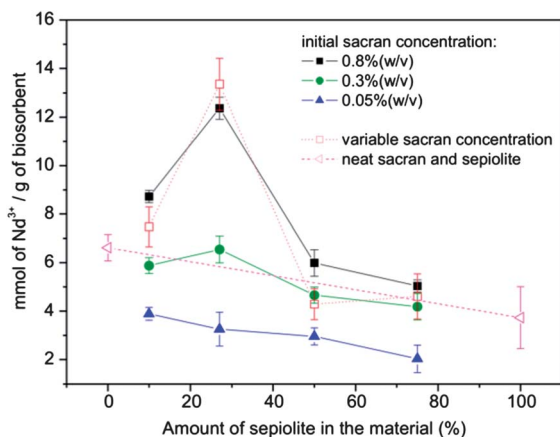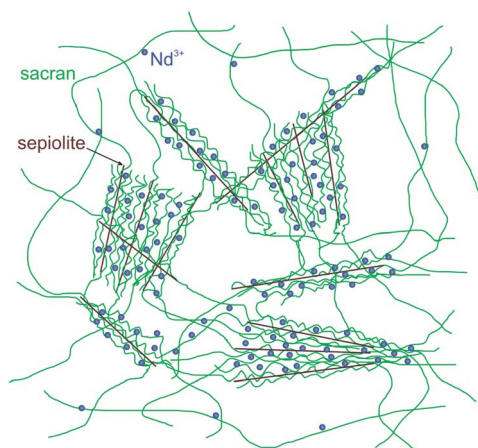
Fig. 8 Comparison of neodymium uptake by sacran–sepiolite bionanocomposites where the initial concentration of sacran is fixed at 0.05, 0.3 or 0.8% (w/v) for each set of samples. For comparison, the dashed lines show some of the results previously collected in Fig. 7, as well as the uptake values for neat sacran and sepiolite.

Scheme 1 Possible arrangement of the sacran chains in liquid crystal domains in sacran–sepiolite samples favouring the Nd^{3+} ion uptake.

uptake was reduced for all the bionanocomposites prepared from diluted sacran solutions, where sacran chains would be arranged as gels (0.3% (w/v)) or in a random-coil conformation (0.05% (w/v)),[9] yielding lower amounts of adsorbed neodymium than the neat sacran and sepiolite samples in the latter case. The assembly with sepiolite at a sacran : clay mass ratio close to 73 : 27 seemed to most likely preserve the liquid crystal orientation of the chains providing the most favourable arrangement for complexing the Nd^{3+} ions, which would lead to high neodymium uptake (Scheme 1). An additional result that supported this hypothesis was the fact that sacran–sepiolite samples (73 : 27 mass ratio) prepared by mixing 0.8% (w/v) sacran and sepiolite by ultrasonication (applied energy 10 kJ) instead of magnetic stirring showed very low values of adsorbed neodymium (Fig. S7†), quite similar to those measured for the samples prepared from diluted sacran (0.05% (w/v)) (Fig. 8). This behaviour may be due to the great disaggregation of sacran chains and sepiolite fibres induced by ultrasound radiation,

similarly to that observed for carbon nanotube-sepiolite systems homogenized by ultrasonication.[40] Under such conditions, the close assembly of the highly disaggregated components would impede the re-organization of the sacran chains in the liquid crystalline state, leading to reduced retention of Nd^{3+} in contrast to the high uptake afforded by the same type of sacran–sepiolite material prepared by magnetic stirring.

Conclusions

Novel bionanocomposite materials were prepared by assembling the cyanobacterial polysaccharide sacran and the fibrous silicate sepiolite. The high affinity and strong interactions between both components as well as the good mechanical and thermal properties of the resulting bionanocomposites were confirmed using diverse characterization techniques. These materials were easily processed as self-supporting films showing a high resistance after immersion in water. The ability of these materials to adsorb lanthanide ions was confirmed. Bionanocomposites prepared from starting sacran solutions of high concentration, >0.5% (w/v), and with a sepiolite content up to *ca.* 43% (w/w) in the final material proved their efficacy in the uptake of neodymium, showing a maximum adsorption of 13.4 mmol of Nd^{3+} per g for the sample containing 27% (w/w) of sepiolite. The preservation of the self-orientation of sacran chains in the liquid crystalline state after assembling with the sepiolite fibres was proposed as the origin of such enhanced adsorption. Several protocols were followed to avoid the formation of the crystalline domains, for instance by decreasing the starting sacran concentration or alternatively by using ultrasound irradiation for the bionanocomposite preparation, leading in all cases to a reduced Nd(III) uptake, which indirectly supports the hypothesis of the key role of liquid crystalline domains in the adsorption process. Thus, the prepared sacran–sepiolite bionanocomposites could be of great interest as biosorbents for the selective recovery of neodymium ions from aqueous solutions. This approach could be an alternative option to respond to the increasing commercial demand of neodymium in view of its large and significant domain of applications in advanced devices.

Acknowledgements

Notes and references

1 M. Darder, P. Aranda and E. Ruiz-Hitzky, *Adv. Mater.*, 2007, **19**, 1309.

2 E. Ruiz-Hitzky, P. Aranda and M. Darder, in *Kirk-Othmer Encyclopedia of Chemical Technology*, John Wiley & Sons, Hoboken, NJ, 2008, p. 1.

1398 | *J. Mater. Chem. A*, 2014, **2**, 1391–1399

This journal is © The Royal Society of Chemistry 2014

3 E. Ruiz-Hitzky, M. Darder and P. Aranda, in *Annual Review of Nanoresearch*, ed. G. Cao, Q. Zhang and C. J. Brinker, World Scientific Publishing, Singapore, 2010, p. 149.

4 M. R. Karim, H. W. Lee, R. Kim, B. C. Ji, J. W. Cho, T. W. Son, W. Oh and J. H. Yeum, *Carbohydr. Polym.*, 2009, **78**, 336.

5 E. Ruiz-Hitzky, M. Darder, P. Aranda, M. Á. Martin del Burgo and G. del Real, *Adv. Mater.*, 2009, **21**, 4167.

6 L. Averous and E. Pollet, *MRS Bull.*, 2011, **36**, 703.

7 M. Okajima-Kaneko, M. Ono, K. Kabata and T. Kaneko, *Pure Appl. Chem.*, 2007, **79**, 2039.

8 M. K. Okajima, S. Miyazato and T. Kaneko, *Langmuir*, 2009, **25**, 8526.

9 M. K. Okajima, D. Kaneko, T. Mitsumata, T. Kaneko and J. Watanabe, *Macromolecules*, 2009, **42**, 3057.

10 *Developments in Palygorskite-Sepiolite Research. A new Outlook on these Nanomaterials*, ed. E. Galán and A. Singer, Elsevier B.V., Oxford, UK, 2011.

11 E. Ruiz-Hitzky, *J. Mater. Chem.*, 2001, **11**, 86.

12 E. Ruiz-Hitzky, P. Aranda, A. Alvarez, J. Santarén and A. Esteban-Cubillo, in *Developments in Palygorskite-Sepiolite Research. A New Outlook on these Nanomaterials*, ed. E. Galán and A. Singer, Elsevier B.V., Oxford, UK, 2011, p. 393.

13 E. Ruiz-Hitzky and A. Van Meerbeek, in *Handbook of clay science. Development in clay science*, ed. F. Bergaya, B. K. G. Theng and G. Lagaly, Elsevier, Amsterdam, 2006, p. 583.

14 E. Ruiz-Hitzky, M. Darder, F. M. Fernandes, B. Wicklein, A. C. S. Alcântara and P. Aranda, *Prog. Polym. Sci.*, 2013, **38**, 1392.

15 F. M. Fernandes, I. Manjubala and E. Ruiz-Hitzky, *Phys. Chem. Chem. Phys.*, 2011, **13**, 4901.

16 Z. Aksu, *Process Biochem.*, 2005, **40**, 997.

17 K. Vijayaraghavan and Y.-S. Yun, *Biotechnol. Adv.*, 2008, **26**, 266.

18 R. De Philippis, G. Colica and E. Micheletti, *Appl. Microbiol. Biotechnol.*, 2011, **92**, 697.

19 M. L. Merroun, K. Ben Chekroun, J. M. Arias and M. T. Gonzalez-Muñoz, *Chemosphere*, 2003, **52**, 113.

20 M. K. Okajima, M. Nakamura, T. Mitsumata and T. Kaneko, *Biomacromolecules*, 2010, **11**, 1773.

21 M. K. Okajima, T. Higashi, R. Asakawa, T. Mitsumata, D. Kaneko, T. Kaneko, T. Ogawa, H. Kurata and S. Isoda, *Biomacromolecules*, 2010, **11**, 3172.

22 M. K. Okajima, A. Kumar, A. Fujiwara, T. Mitsumata, D. Kaneko, T. Ogawa, H. Kurata, S. Isoda and T. Kaneko, *Biopolymers*, 2013, **99**, 1.

23 T. G. Goonan, *U.S. Geological Survey Scientific Investigations Report 2011-5094*, 2011.

24 S. V. Eliseeva and J.-C. G. Buenzli, *New J. Chem.*, 2011, **35**, 1165.

25 L. Friebe, O. Nuyken and W. Obrecht, in *Neodymium Based Ziegler Catalysts-Fundamental Chemistry*, ed. O. Nuyken, Springer-Verlag, Heidelberg, 2006, p. 1.

26 M. K. Okajima, T. Bamba, Y. Kaneso, K. Hirata, E. Fukusaki, S. I. Kajiyama and T. Kaneko, *Macromolecules*, 2008, **41**, 4061.

27 A. Seeboth and H. R. Holzbauer, *Adv. Mater.*, 1996, **8**, 408.

28 C. H. Giles, T. H. MacEwan, S. N. Nakhwa and D. Smith, *J. Chem. Soc.*, 1960, 3973.

29 M. Darder, M. Lopez-Blanco, P. Aranda, A. J. Aznar, J. Bravo and E. Ruiz-Hitzky, *Chem. Mater.*, 2006, **18**, 1602.

30 A. C. S. Alcântara, M. Darder, P. Aranda and E. Ruiz Hitzky, *Eur. J. Inorg. Chem.*, 2012, **2012**, 5216.

31 W. X. Kuang, G. A. Facey, C. Detellier, B. Casal, J. M. Serratosa and E. Ruiz-Hitzky, *Chem. Mater.*, 2003, **15**, 4956.

32 S. Balci, *J. Chem. Technol. Biotechnol.*, 1996, **66**, 72.

33 M. Alexandre and P. Dubois, *Mater. Sci. Eng., R*, 2000, **28**, 1.

34 G. A. Fugate, Ph.D. Thesis, Florida State University, 2004.

35 R. C. Oliveira, E. Guibal and O. Garcia, Jr, *Biotechnol. Prog.*, 2012, **28**, 715.

36 Y. Takahashi, K. Kondo, A. Miyaji, M. Umeo, T. Honma and S. Asaoka, *Anal. Sci.*, 2012, **28**, 985.

37 F. Wang, J. Zhao, H. Zhou, W. Li, N. Sui and H. Liu, *J. Chem. Technol. Biotechnol.*, 2013, **88**, 317.

38 R. Qadeer, *J. Radioanal. Nucl. Chem.*, 2005, **265**, 377.

39 C. Xiong, X. Chen and C. Yao, *J. Rare Earths*, 2011, **29**, 979.

40 F. M. Fernandes, Ph.D. Thesis, Autonomous University of Madrid, 2011.

This journal is © The Royal Society of Chemistry 2014

J. Mater. Chem. A, 2014, **2**, 1391–1399 | **1399**